

Evidence for a Lower Value for H_0 from Cosmic Chronometers Data?

Vinicius C. Busti^{1*}, Chris Clarkson¹ and Marina Seikel^{2,1}

¹ *Astrophysics, Cosmology & Gravity Centre (ACGC), and*

Department of Mathematics and Applied Mathematics, University of Cape Town, Rondebosch 7701, Cape Town, South Africa

² *Physics Department, University of Western Cape, Cape Town 7535, South Africa*

Accepted . Received ; in original form

ABSTRACT

An intriguing discrepancy emerging in the concordance model of cosmology is the tension between the locally measured value of the Hubble rate, and the ‘global’ value inferred from the cosmic microwave background (CMB). This could be due to systematic uncertainties when measuring H_0 locally, or it could be that we live in a highly unlikely Hubble bubble, or other exotic scenarios. We point out that the global H_0 can be found by extrapolating $H(z)$ data points at high- z down to $z = 0$. By doing this in a Bayesian non-parametric way we can find a model-independent value for H_0 . We apply this to 19 measurements based on differential age of passively evolving galaxies as cosmic chronometers. Using Gaussian processes, we find $H_0 = 64.9 \pm 4.2 \text{ km s}^{-1} \text{ Mpc}^{-1}$ (1σ), in agreement with the CMB value, but reinforcing the tension with the local value. An analysis of possible sources of systematic errors shows that the stellar population synthesis model adopted may change the results significantly, being the main concern for subsequent studies. Forecasts for future data show that distant $H(z)$ measurements can be a robust method to determine H_0 , where a focus in precision and a careful assessment of systematic errors are required.

Key words: cosmological parameters – cosmology: observations – cosmology: theory – dark energy – large-scale structure of Universe – cosmology: distance scale

1 INTRODUCTION

There is a strong tension, recently quantified by Verde et al. (2013), between the value of the Hubble constant H_0 derived by *Planck* (Planck Collaboration 2013) from anisotropies in the cosmic microwave background (CMB): $67.3 \pm 1.2 \text{ km s}^{-1} \text{ Mpc}^{-1}$, and the value from local measurements: $73.8 \pm 2.4 \text{ km s}^{-1} \text{ Mpc}^{-1}$ (Riess et al. 2011). While the latter measurement is based on local measurements, the former infers a global value for the Hubble constant within a cosmological model.

There remains disagreement about the local value of H_0 depending on the distance indicator used to measure it, which hints the discrepancy with *Planck* could be the result of systematic errors. Riess et al. (2011) calibrated the SNe Ia distances with three indicators: distance to NGC 4258 based on a megamaser measurement, parallax measurements to Milk Way cepheids (MWC) and cepheids observations and a revised distance to the Large Magellanic Cloud (LMC). Contrarily, calibrating the SNe Ia with the tip of red-giant branch, Tammann & Reindl (2013) provides $H_0 = 63.7 \pm 2.3 \text{ km s}^{-1} \text{ Mpc}^{-1}$. This shows how crucial is the first-step calibration in the distance ladder to measure H_0 .

However, there are several local H_0 measurements with higher values. Riess et al. (2012) found $H_0 = 75.4 \pm 2.9 \text{ km s}^{-1} \text{ Mpc}^{-1}$ by using cepheids in M31. With a mid-infrared calibration for the cepheids, Freedman et al. (2012) derived $H_0 = 74.3 \pm 2.1 \text{ km s}^{-1} \text{ Mpc}^{-1}$, and with 8 new classical cepheids observed in galaxies hosting SNe Ia Fiorentino et al. (2013) got $H_0 = 76.0 \pm 1.9 \text{ km s}^{-1} \text{ Mpc}^{-1}$. By using HII regions and HII galaxies as distance indicators, Chávez et al. (2012) obtained $H_0 = 74.3 \pm 3.1(\text{random}) \pm 2.9(\text{syst.}) \text{ km s}^{-1} \text{ Mpc}^{-1}$. Some of these are over 4σ away from the CMB-derived value. See Fig. 1 for a plot of different measurements of H_0 .

A variety of different physical effects could explain such a discrepancy. It could just be cosmic variance: as we can observe the Universe from only one position, we are not able to realize the global parameters from the local parameters, as in the local expansion rate for instance. If we live in a locally underdense region, a ‘Hubble bubble’, a higher value for H_0 is obtained compared to the global value. This effect was carefully addressed by Marra et al. (2013) through a modelling of the statistics of matter distribution which provides the distribution of the gravitational potential at the observer. The outcome is that cosmic variance can alleviate the tension, but a complete elimination requires a very rare fluctuation (Marra et al. 2013; Wojtak et al. 2014).

* E-mail: vinicius.busti@uct.ac.za

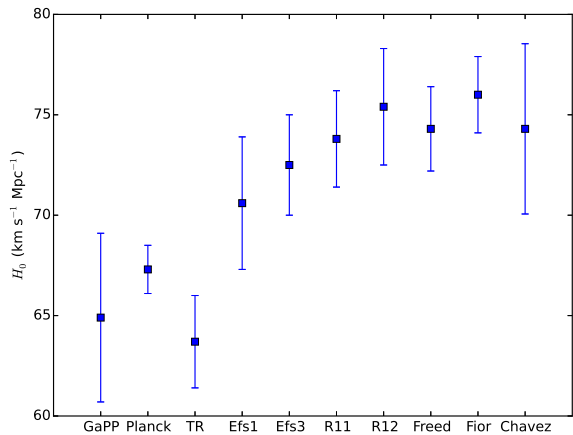


Figure 1. *Different measurements of H_0 .* The figure shows how the result obtained in this work (GaPP) is compared to other determinations of H_0 . The points refer to the following references: Planck (Planck Collaboration 2013), TR (Tammann & Reindl 2013), Efs1 (Efstathiou 2013) with one anchor, Efs3 with three anchors, R11 (Riess et al. 2011), R12 (Riess et al. 2012), Freed (Freedman et al. 2012), Fior (Fiorentino et al. 2013) and Chavez (Chávez et al. 2012).

Another way to look at the problem is to consider that the discrepancy may indicate new physics, such as massive neutrinos (Wyman et al. 2014), or alternative dark energy models (Salvatelli et al. 2013; Xia et al. 2013).

Recently, some analyses were performed trying to identify sources of systematic errors in order to remove or alleviate the tension. For example, by using only the geometric maser distance to NGC 4258 of Humphreys et al. (2013) as an anchor, Efstathiou (2013) revisited Riess et al. (2011) analysis and derived $H_0 = 70.6 \pm 3.3$ km s $^{-1}$ Mpc $^{-1}$, while combining with LMC and MWC anchors the value is 72.5 ± 2.5 km s $^{-1}$ Mpc $^{-1}$, alleviating the tension. The *Planck* data were also reanalysed by Spergel et al. (2013), where it was claimed that the 217 GHz \times 217 GHz detector is responsible for some part of the tension. Their new Hubble constant without the 217 GHz \times 217 GHz detector is slightly higher: $H_0 = 68.0 \pm 1.1$ km s $^{-1}$ Mpc $^{-1}$.

With so many alternatives, progress can be achieved by developing new ways to address the issue. We point out here that $H(z)$ data which are not calibrated on a H_0 estimate can be extrapolated to $z=0$ to provide an independent measurement of the global H_0 . Here, the Hubble function is reconstructed in order to derive H_0 from 19 $H(z)$ measurements of passively evolving galaxies as cosmic chronometers (Jimenez & Loeb 2002). Many of these are at relatively moderate and high redshifts so intrinsically probe the global value for H_0 rather than the local one. We use Gaussian Processes (GP), which is a non-parametric method, to obtain the value of the Hubble constant in a completely cosmological model-independent way, which is in principle not affected by the local systematics. We show the value of the Hubble constant derived in this way is lower than the standard local measurements. We obtain $H_0 = 64.9 \pm 4.2$ km s $^{-1}$ Mpc $^{-1}$ (1σ), in agreement with the CMB-inferred value. A better understanding of systematic errors, especially the adopted

stellar population synthesis model, is required: we show that to improve this result a big effort is necessary to decrease the errors substantially in future, and a focus on precision is worthier than the number of data.

The paper is organized as follows: in Sec. 2 we describe GP as well as standard parametric methods adopted to constrain H_0 . In Sec. 3 the bounds derived for the Hubble constant are displayed, followed by forecasts of constraints in Sec. 4. We finish the paper in Sec. 5 with the conclusions.

2 METHODS

2.1 Gaussian Processes (GP)

A gaussian *distribution* is a distribution over random variables, while a gaussian *process* is a distribution over functions. This allows one to reconstruct a function from data without assuming a parametrisation for it. Here we use GaPP (Gaussian Processes in Python)¹ (Seikel et al. 2012) in order to reconstruct the Hubble parameter as a function of the redshift from which we can infer H_0 . This method has been applied for several purposes, for example the reconstruction of the equation of state of dark energy (Seikel et al. 2012) and to perform null tests of the concordance model (Seikel et al. 2012b; Yahya et al. 2013).

The reconstruction is given by a mean function with gaussian error bands, where the function values at different points z and \tilde{z} are connected through a covariance function $k(z, \tilde{z})$ (see Seikel & Clarkson (2013) for a discussion of choices of covariance functions). This covariance function depends on a set of hyperparameters. Here, as we expect that the Hubble parameter and all its derivatives to be smooth, we consider the general purpose squared exponential (Sq. Exp.) covariance function which is given by

$$k(z, \tilde{z}) = \sigma_f^2 \exp \left\{ -\frac{(z - \tilde{z})^2}{2l^2} \right\}. \quad (1)$$

In the above equation we have two hyperparameters, the first σ_f is related to typical changes in the function value while the second l is related to the distance one needs to move in input space before the function value changes significantly. We follow the steps of Seikel et al. (2012) and determine the maximum likelihood value for σ_f and l in order to obtain the value of the function. In this way, we are able to reconstruct the Hubble parameter as a function of the redshift from $H(z)$ measurements. We discuss in Sect. 3.1.1 the impact of different covariance functions on our results.

2.2 Parametric Analyses

In order to compare the results provided by non-parametric methods with standard analyses, we also consider two parametric models. First of all, we take a flat Λ CDM model, where the universe is composed by dark matter and a fluid X with equation of state $p_X = w\rho_X$, where the Hubble parameter is given by

$$H(z) = H_0 \sqrt{\Omega_m(1+z)^3 + (1 - \Omega_m)(1+z)^{3(1+w)}}, \quad (2)$$

¹ <http://www.acgc.uct.ac.za/~seikel/GAPP/index.html>

Table 1. H_0 constraints from 19 $H(z)$ measurements.

Method	$H_0 \pm 1\sigma$ (km s ⁻¹ Mpc ⁻¹)	σ_{H_0} (km s ⁻¹ Mpc ⁻¹)
Sq. Exp.	64.9	4.2
Matérn(9/2)	65.9	4.5
Matérn(7/2)	66.4	4.7
Matérn(5/2)	67.4	5.2
Λ CDM	68.9	2.8
XCDM	69.0	6.7

where Ω_m is the matter density parameter today. When $w = -1$ this is the concordance Λ CDM model which we consider separately. In order to derive H_0 for the parametric models, we apply standard statistical procedures based on maximum likelihood methods.

3 CONSTRAINTS ON H_0

We use 19 $H(z)$ measurements (Simon et al. 2005; Stern et al. 2010; Moresco et al. 2012) from passively evolving galaxies as cosmic chronometers to derive the value of H_0 .

Figure 2 presents the results for the non-parametric approach adopted in this work. We also plot the $H(z)$ measurements with their respective errorbars. The blue solid line refers to the reconstruction with GaPP, with the shaded contours designating the 1σ errors. When extrapolated to redshift $z = 0$, we obtain $H_0 = 64.9 \pm 4.2$ km s⁻¹ Mpc⁻¹ (1σ). Note that this value is completely independent of a cosmological model, which makes it complementary but consistent with the *Planck* value which is derived within the Λ CDM model. In this way, our result can also be used to shed light in the whole cosmological model. This result goes in the direction of a model-independent approach with SNe Ia which also prefers lower values for H_0 (Benitez-Herrera et al. 2013).

As a means to compare the non-parametric with standard parametric analyses, a flat Λ CDM model and a flat XCDM are also considered. The Hubble constant is found to be $H_0 = 68.9 \pm 2.8$ km s⁻¹ Mpc⁻¹ (1σ) for the flat Λ CDM model and $H_0 = 69.0 \pm 6.7$ km s⁻¹ Mpc⁻¹ (1σ) for XCDM. The bigger error for the XCDM case is derived as a consequence of the inclusion of an extra parameter. The mean values are higher compared to the non-parametric approach, and in closer agreement with locally measured values, but also in agreement with the non-parametric result.

Table 1 summarizes the constraints for H_0 with 1σ errors. All methods prefer values for H_0 below 70 km s⁻¹ Mpc⁻¹, in contrast with some local determinations of H_0 .

3.1 Systematic Errors

Some tests were performed in order to evaluate the robustness of the result. We split our analysis searching for three effects: (i) the impact of the covariance function in GaPP, (ii) a possible presence of outliers driving H_0 for lower values and (iii) systematic errors from the stellar population synthesis (SPS) models.

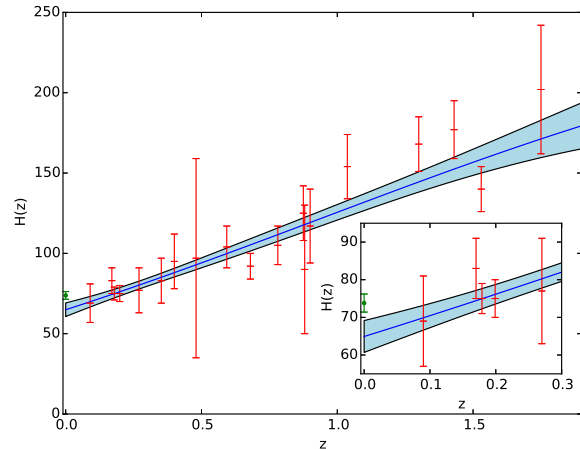


Figure 2. Model independent reconstruction of $H(z)$ using Gaussian processes. The red points with error bars represent the 19 $H(z)$ measurements and the blue shaded contour the reconstruction within the 1σ confidence level. For comparison purposes, we also show the value obtained by Riess et al. (2011), where we see that it is compatible to the GaPP value only at 2σ . The inset shows a zoom in the low redshift region.

3.1.1 Covariance Functions

The freedom in the GP approach comes in the covariance function. While in traditional parametric analyses we choose a model to characterise what is our prior belief about the function in which we are interested, with GP we ascribe in the covariance function our priors about the expected function properties (e.g. smoothness, correlation scales etc.).

Since we expect the Hubble parameter and its derivatives to be smooth, the squared exponential covariance function was selected which is infinitely differentiable – this implies that functions drawn from the process are also infinitely differentiable. However, we considered other covariance functions to see how the results are affected. In order to do so, we considered three covariance functions from the Matérn family, namely the $\nu = 5/2$, $7/2$ and $9/2$ (see Seikel & Clarkson (2013) for definitions and further discussion). Writing $\nu = p + 1/2$, each Matérn function is p times differentiable as are functions drawn from it, and the squared exponential is recovered for $\nu \rightarrow \infty$. Increasing ν increases the width of the covariance function near the peak implying stronger correlations from nearby points for a fixed correlation length ℓ .

The results are shown in Table 1, where we see slightly higher values are derived for H_0 , together with slightly larger errors, for smaller ν . In fact, for the Matérn(5/2) the tension with local H_0 disappears, although the result remains in fully agreement with *Planck*. Interestingly, although there is some shift, the errors are relatively independent of the covariance function choice, especially when compared to the ones derived when one increases the number of parameters in parametric analyses (the error more than doubles when allowing for w to be free, compared to fixing it to -1), showing that GP provide very stable results within different reasonable assumptions.

3.1.2 Presence of Outliers

We checked if the high-redshift data were pivoting down the value of H_0 to smaller values. To do so, we removed all data points with redshifts greater than 1, but again the results were completely consistent with the full sample, $H_0 = 66.9 \pm 4.3 \text{ km s}^{-1} \text{ Mpc}^{-1}$, thus not removing the tension. By removing low-redshift points, first and second or third and fourth, again the results did not change significantly, with $H_0 = 66.3 \pm 4.6 \text{ km s}^{-1} \text{ Mpc}^{-1}$ and $H_0 = 66.4 \pm 7.1 \text{ km s}^{-1} \text{ Mpc}^{-1}$, respectively. We note that the points with smaller errors dominate the final error budget, as confirmed also by the analysis done in Sect. 4.

We also removed point by point in the analysis. For the first 17 points, the results changed slightly, with a mean value between 64 and 65 and errors between 4 and 5. Conversely, the high-redshift points showed the biggest departure once removed, with values $H_0 = 71.5 \pm 5.9$ (18th out) and $H_0 = 73.2 \pm 8.7 \text{ km s}^{-1} \text{ Mpc}^{-1}$ (19th out). Higher values are derived and the error blows up, although in agreement with the full sample. This shows how H_0 is sensitive to high-redshift values, where more data points in this redshift region might help to mitigate possible systematic errors due to outliers.

3.1.3 Different SPS Models

One of the possible main sources of systematic errors in $H(z)$ measurements comes from the adopted SPS model. The 19 points used here were derived with Bruzual & Charlot (2003) SPS model (BC03). On the other hand, recently Moresco et al. (2012) calculated $H(z)$ for eight measurements considering BC03 and another SPS model from Maraston & Stromback (2011, MaStro). We performed the reconstruction with GaPP for this subset with both SPS models. For BC03 we derived H_0 in the range $64.4 \pm 4.9 \text{ km s}^{-1} \text{ Mpc}^{-1}$, in good agreement with the full sample. On the contrary, the analysis with MaStro provided $H_0 = 75.1 \pm 5.2 \text{ km s}^{-1} \text{ Mpc}^{-1}$, in disagreement with *Planck* and in good agreement with the value of Riess et al. (2011). Therefore, even with only eight data points, we identify the SPS model as the main concern for our results.

3.2 Other Data Sets

Another independent measurement for $H(z)$ is given by baryon acoustic oscillations (BAOs). Currently, there are 7 measurements from Blake et al. (2012), Reid et al. (2012), Xu et al. (2013), Busca et al. (2013) and Chuang & Wang (2013). Combining with the other measurements, for GaPP (Sq. Exp.) we got $H_0 = 69.4 \pm 4.4 \text{ km s}^{-1} \text{ Mpc}^{-1}$, for a flat Λ CDM model $H_0 = 68.4 \pm 2.0 \text{ km s}^{-1} \text{ Mpc}^{-1}$ and for a flat XCDM model $H_0 = 69.8 \pm 4.6$, all values consistent with *Planck*. However, there are some drawbacks when using the BAO data. First, these data are not model independent. They are based on the Λ CDM model to study the correlation functions and transform them to the $H(z)$ values. Moreover, generally what is inferred is the combination Hr_s , r_s standing for the sound horizon whose value is given by *WMAP* (Komatsu et al. 2009, 2011; Hinshaw et al. 2013). Also important is the point raised by Blake et al. (2012) warning

that their values of $H(z)$ are derived and so they should not be used to test models.

Since the current errors do not allow a final decision about the value of H_0 , our next step is to study whether future data can settle the issue.

4 FORECASTS

The procedure to analyse how future data can improve the determination of H_0 is split in two ways. First, we consider how the increase of data points of same quality can change the constraints. Second, the errors for $H(z)$ are shrunk and a comparison is made between the number of data and their quality.

The current errors for $H(z)$ measurements grow with redshift a few percent up to around 15 per cent. Assuming that future data will provide measurements with the same errors, we update the method of Ma & Zhang (2011) to predict future data based on the recent measurements from Moresco et al. (2012). A value for $H(z)$ is generated by $H_{sim}(z) = H_{fid}(z) + \mathcal{N}(0, \bar{\sigma}(z))$, where $H_{sim}(z)$ and $H_{fid}(z)$ are respectively the simulated and fiducial values for the Hubble parameter at redshift z , and $\mathcal{N}(0, \bar{\sigma}(z))$ is a random number gaussianly distributed with mean zero and variance $\bar{\sigma}(z)$. To estimate $\bar{\sigma}(z)$, the uncertainties of the observational points are restricted by two straight lines: $\sigma_+ = 15.76z + 3.65$ and $\sigma_- = 13.29z + 1.62$, with two “outliers” removed since they were not following the trend of the errors. Assuming that the errors of future data will be between the two lines, one can expect the mean line of the error to be $\sigma_0 = 14.52z + 2.63$. Therefore, the error of the simulated point is drawn from a gaussianly distributed random variable $\bar{\sigma}(z) = \mathcal{N}(\sigma_0(z), \epsilon(z))$, where $\epsilon(z) = (\sigma_+ - \sigma_-)/4$ is chosen to assure the error is within σ_- and σ_+ with 95.4% probability.

Figure 3 presents the expected future errors from considering data are equally spaced in the interval $0.1 \leq z \leq 1.8$. We present the expected error on H_0 from simulations with 64, 128, and 256 data points. These numbers were chosen because with 64 $H(z)$ measurements of same quality as today one can achieve the same constraints given by current SNe Ia (Ma & Zhang 2011). The black crosses represent the errors with the GaPP reconstruction, the red dots for the flat XCDM model and the blue triangles for the flat Λ CDM model. The first panel in the left shows the behavior of future data with the same quality as today, and the others show the trend for smaller errors for the $H(z)$ data, of 10%, 5%, and 3% (see Crawford et al. (2010) for an observational program to achieve such values).

Some conclusions can be made from Fig. 3:

- For future data with the same quality as today GaPP performs very well, with errors smaller than the ones obtained with a flat XCDM model.
- Current quality data provide better constraints to H_0 than a constant error of 10% in the whole redshift range, showing that lower redshift objects with higher precision compensate the low quality data at high redshifts.
- For higher precision measurements GaPP and the XCDM model provide the same constraints, showing that a non-parametric approach is powerful to study cosmological data.

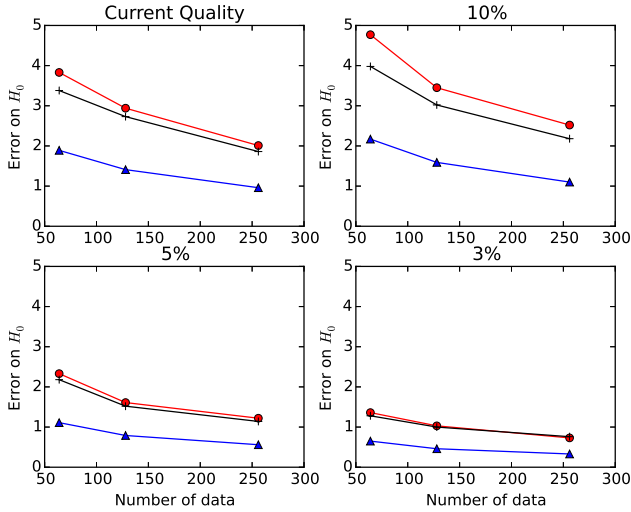


Figure 3. Forecasts for errors on H_0 (in $\text{km s}^{-1} \text{Mpc}^{-1}$) with different number of data points. The future data is evenly spaced in the redshift range $0.1 \leq z \leq 1.8$. The black crosses refer to the error provided by GaPP, while the red points refer to a flat XCDM model and the blue triangles to a flat Λ CDM model. The upper left panel refers to simulated data with the same quality as current data. The upper right panel for simulated data with 10% precision, the lower left with 5% and the lower right with 3% precision.

- Improvement in precision is more important than increasing the number of data of poorer quality.

5 CONCLUSIONS

We have applied GaPP, a non-parametric smoothing method based on Gaussian Processes, to 19 $H(z)$ measurements in order to constrain the Hubble constant H_0 . This method does not rely on a cosmological model, so its results can be used to infer the impact of systematic errors as well as the underlying cosmological framework. We have obtained H_0 to be $64.9 \pm 4.2 \text{ km s}^{-1} \text{Mpc}^{-1}$ (1σ), a value which is in agreement with *Planck*, but in disagreement with local measurements. This supports the notion that either there are unidentified systematic errors in the local H_0 data, or the local value is indeed different from the global value. A better comprehension of systematic errors, especially a thorough analysis of the impact of SPS models, can improve the robustness of our results. Simulations have shown that improvements in distant $H(z)$ measurements can help pin down the global value of H_0 .

ACKNOWLEDGMENTS

The authors are grateful to Raul Jimenez and Martin Hendry for useful comments. VCB is supported by CNPq-Brazil through a fellowship within the program Science without Borders. MS is supported by the South Africa Square Kilometre Array Project and the South African National Research Foundation (NRF).

REFERENCES

- Benitez-Herrera S., Ishida E. E. O., Maturi M., Hillebrandt W., Bartelmann M., Röpke F., 2013, MNRAS, 436, 854
 Busca N. G. et al., 2013, A&A, 552, 96
 Blake C. et al., 2012, MNRAS, 425, 405
 Bruzual G., Charlot S., 2003, MNRAS, 344, 1000
 Chávez R., Terlevich E., Terlevich R., Plionis M., Bresolin F., Basilakos S., Melnick J., 2012, MNRAS, 425, L56
 Crawford S. M., Ratsimbazafy A. L., Cress C. M., Olivier E. A., Blyth S.-L., van der Heyden K. J., 2010, MNRAS, 406, 2569
 Chuang C.-H., Wang, Y., 2013, MNRAS, 435, 255
 Efsthathiou G., 2013, preprint(arXiv:1311.3461)
 Fiorentino G., Musella I., Marconi M., 2013, MNRAS, 434, 2866
 Freedman W. L., Madore B. F., Scowcroft V., Burns C., Monson A., Persson S. E., Seibert M., Rigby J., 2012, ApJ, 758, 24
 Hinshaw G. et al., 2013, ApJS, 208, 19
 Humphreys E. M. L., Reid M. J., Moran J. M., Greenhill L. J., Argon A. L., 2013, ApJ, 775, 13
 Jimenez R., Loeb A., 2002, ApJ, 573, 37
 Komatsu E. et al., 2009, ApJS, 180, 330
 Komatsu E. et al., 2011, ApJS, 192, 18
 Ma C., Zhang T.-J., 2011, ApJ, 730, 74
 Maraston C., Stromback G., 2011, MNRAS, 418, 2785
 Marra V., Amendola L., Sawicky I., Valkenburg W., 2013, Phys. Rev. Lett., 110, 241305
 Moresco M. et al., 2012, J. Cosmol. Astropart. Phys., 8, 6
 Planck Collaboration, 2013, preprint(arXiv:1303.5076)
 Reid B. A. et al., 2012, MNRAS, 426, 2719
 Riess A. G. et al., 2011, ApJ, 730, 119
 Riess A. G., Fliri J., Valls-Gabaud D., 2012, ApJ, 745, 156
 Salvatelli V., Marchini A., Lopez-Honores L., Mena O., 2013, Phys. Rev. D, 88, 023531
 Seikel M., Clarkson C., Smith M., 2012, J. Cosmol. Astropart. Phys., 6, 36
 Seikel M., Yahya S., Maartens R., Clarkson C., 2012, Phys. Rev. D, 86, 083001
 Seikel M., Clarkson C., 2013, preprint(arXiv:1311.6678)
 Simon J., Verde L., Jimenez R., 2005, Phys. Rev. D, 71, 123001
 Spergel D., Flauger R., Hlozek R., 2013, preprint(arXiv:1312.3313)
 Stern D., Jimenez R., Verde L., Kamionkowski M., Stanford S. A., 2010, J. Cosmol. Astropart. Phys., 2, 8
 Tammann G. A., Reindl B., 2013, A&A, 549, 136
 Verde L., Protopapas P., Jimenez R., 2013, Physics of the Dark Universe, 2, 166
 Xia J.-Q., Li H., Zhang X., 2013, Phys. Rev. D, 88, 063501
 Xu X., Cuesta A. J., Padmanabhan N., Eisenstein D. J., McBride C. K., 2013, MNRAS, 431, 2834
 Yahya S., Seikel M., Clarkson C., Maartens R., Smith M., 2013, preprint(arXiv:1308.4099)
 Wojtak R., Knebe A., Watson W. A., Iliev I. T., Hess S., Rapetti D., Yepes G., Gottloeber S., 2014, MNRAS, 438, 1805
 Wyman M., Rudd D. H., Vanderveld A., Hu W., 2014, Phys. Rev. Lett., 112, 051302